Eur. Phys. J. C 19, 43–55 (2001)
Digital Object Identifier (DOI) 10.1007/s100520100594

THE EUROPEAN PHYSICAL JOURNAL C

High sensitivity 2β decay study of ^{116}Cd and ^{100}Mo with the BOREXINO counting test facility (CAMEO project)

G. Bellini[1], B. Caccianiga[1], M. Chen[3], F.A. Danevich[2], M.G. Giammarchi[1], V.V. Kobychev[2], B.N. Kropivyansky[2], E. Meroni[1], L. Miramonti[1], A.S. Nikolayko[2], L. Oberauer[4], O.A. Ponkratenko[2], V.I. Tretyak[2], S.Yu. Zdesenko[2], Yu.G. Zdesenko[2,a]

[1] Physics Department of the University and INFN, 20133 Milano, Italy
[2] Institute for Nuclear Research, MSP 03680 Kiev, Ukraine
[3] Department of Physics, Queen's University, Kingston, Canada
[4] Technical University Munich, Garching, Germany

Received: 20 July 2000 / Revised version: 9 January 2001 /
Published online: 23 February 2001 – © Springer-Verlag 2001

Abstract. The unique features (super-low background and large sensitive volume) of the CTF and BOREXINO set ups are used in the CAMEO project for a high sensitivity study of ^{100}Mo and ^{116}Cd neutrinoless 2β decay. Pilot measurements with ^{116}Cd and Monte Carlo simulations show that the sensitivity of the CAMEO experiment (in terms of the half-life limit for $0\nu2\beta$ decay) is $\approx 4\times10^{24}$ yr with a 1 kg source of ^{100}Mo and $\approx 10^{26}$ yr with $\approx$100 kg of enriched $^{116}CdWO_4$ crystals placed in the liquid scintillator of the CTF. The last value corresponds to a limit on the neutrino mass of $m_\nu \leq 0.06$ eV. Similarly with 1000 kg of $^{116}CdWO_4$ crystals located in the BOREXINO apparatus the neutrino mass limit can be pushed down to $m_\nu \leq 0.02$ eV.

1 Introduction

Neutrinoless double beta ($0\nu2\beta$) decay is forbidden in the Standard Model (SM) since it violates lepton number (L) conservation. However many extensions of the SM incorporate L violating interactions and thus could lead to $0\nu2\beta$ decay [1,2]. Currently, besides the conventional left-handed neutrino (ν) exchange mechanism, there are many other possibilities to trigger this process [2]: right-handed ν exchange in left-right symmetric models; exchange of squarks, sneutrinos, etc. via supersymmetric (SUSY) interactions; exchange of leptoquarks in models with leptoquarks; exchange of excited Majorana neutrinos in models with composite heavy neutrinos, and so on. In that sense $0\nu2\beta$ decay has a great conceptual importance due to the strong statement obtained in a gauge theory of the weak interaction that a non-vanishing $0\nu2\beta$ decay rate requires neutrinos to be massive Majorana particles, independently of which mechanism induces it [3]. Therefore, at present $0\nu2\beta$ decay is considered as a powerful method to test new physical effects beyond the SM, while absence of this process – established at the present level of sensitivity – would yield strong restrictions on parameters of manifold extensions of the SM and narrow the wide choice of the theoretical models. At the same time $0\nu2\beta$ decay is very important in light of the current status of neutrino physics (see [4]). Indeed, the solar neutrino problem (in particular lack of ^{7}Be neutrinos) and the deficit of the atmospheric muon neutrino flux [5] could be explained by means of neutrino oscillations, which require nonzero neutrino masses. Also indication for ν_μ/ν_e oscillations was found by the LSND collaboration [4,6]. Oscillation experiments are only sensitive to neutrino mass difference, while measuring the $0\nu2\beta$ decay rate can give the absolute scale[1] of the effective Majorana ν mass, and hence provide a crucial test of neutrino mass models.

Despite the numerous efforts to observe $0\nu2\beta$ decay beginning from 1948 up to the present [1] this process still remains unobserved. The highest half-life limits were set in direct experiments with several nuclides: $T_{1/2}(0\nu) \geq 10^{22}$ yr for ^{82}Se [7], ^{100}Mo [8]; $T_{1/2}(0\nu) \geq 10^{23}$ yr for ^{116}Cd [9, 10], ^{130}Te [11] and ^{136}Xe [12]; and $T_{1/2}(0\nu) \geq 10^{25}$ yr for ^{76}Ge [13,14].

These results have already brought the most stringent restrictions on the values of the Majorana neutrino mass $m_\nu \leq (0.5 - 2.5)$ eV, right-handed admixtures in weak interaction $\eta \approx 10^{-7}$, $\lambda \approx 10^{-5}$, and the neutrino-Majoron coupling constant $g_M \approx 10^{-4}$ (see, however, footnote 1). At the same time, on the basis of current theoretical and experimental status of astroparticle physics (and neutrino physics in particular) it is very desirable to improve far-

[a] *Corresponding author.* Address: Institute for Nuclear Research, prospect Nauki 47, MSP 03680 Kiev, Ukraine
(e-mail: zdesenko@kinr.kiev.ua)

[1] Obviously, its accuracy depends on the uncertainties of the nuclear matrix elements calculation

ther the present level of sensitivity by one-two orders of magnitude [1,2,15–17].

With this aim we consider in the present paper the use of the super-low background liquid scintillation detector – the BOREXINO Counting Test Facility (CTF) [18] – for high sensitivity 2β decay research.

2 The CTF and choice of candidate nuclei

The full description of the CTF and its performance have been published elsewhere [18–20]. Here we recall the main features of this apparatus, which are important in the following.

The CTF is installed in the Gran Sasso Underground Laboratory and consists of an external cylindrical water tank ($\oslash$11×10 m; $\approx$ 1000 t of water) serving as passive shielding for 4.8 m^3 of pseudocumene based liquid scintillator contained in an inner spherical vessel of $\oslash$2.1 m. High purity water is supplied by the BOREXINO water plant, which provides its radio-purity level of $\approx 10^{-14}$ g/g (U, Th), $\approx 10^{-10}$ g/g (K natural) and <5 μBq/l for ^{222}Rn [18,20,21].

The liquid scintillator has the fluorescence peak emission at 365 nm and the yield of emitted photons is $\approx 10^4$ per MeV of energy deposited. The attenuation length is larger than 5 m above 380 nm [22]. The principal scintillator decay time was measured as $\approx$3.5 ns in a small volume, while as 4.5–5.0 ns with a source placed in the center of the CTF. The scintillator is carefully purified which ensures that ^{232}Th and ^{238}U contaminations in it are less than $(2\text{–}5)\cdot 10^{-16}$ g/g.

The inner vessel for the liquid scintillator is made of nylon film, 500 μm thick, with excellent optical clarity at 350–500 nm, which allows collection of scintillation light with the help of 100 phototubes (PMT) fixed to a 7 m diameter support structure inside the water tank. The PMTs are 8$''$ EMI 9351 tubes made of low radioactivity glass, and characterized by high quantum efficiency (26% at 420 nm), limited transit time spread (σ = 1 ns) and good pulse height resolution for single photoelectron pulses (Peak/Valley = 2.5). The PMTs are fitted with light concentrators 57 cm long and 50 cm diameter aperture. They provide 20% optical coverage. The number of photoelectrons per MeV measured experimentally is (300 $\pm$ 30)/MeV on average. Additional nylon barrier against radon convection and a muon veto system were installed in 1999.

For each event the charge and timing (precision of 1 ns) of hit PMTs are recorded. Each channel is doubled by an auxiliary channel to record all other events coming within a time window of 8 ms after the first event. For longer delay the computer clock is used. Event parameters measured in the CTF include:

- the total charge collected by the PMTs during 0–500 ns (event energy);
- the tail charge (48–548 ns) used for pulse shape discrimination;
- PMT timing to reconstruct the event in space (resolution of 10–15 cm);
- the time elapsed between sequential events, used to tag time-correlated events.

Due to all these measures the CTF is the best super-low background scintillator of large volume at present. Indeed, the background rate in the total energy region 250–2500 keV (important for 2β decay study) is about 0.03 counts/yr·keV·kg, while in the energy interval 250–800 keV (so called "solar neutrino energy window") is about 0.3 counts/yr·keV·kg and is dominated by external background from Rn in the shielding water ($\approx$30 mBq/m^3 in the region surrounding the inner vessel). The internal background is less than 0.01 counts/yr·keV·kg in 250–800 keV interval. Therefore one can conclude that the CTF is the ideal apparatus for super-low background 2β decay research.

For the choice of 2β candidate nuclei let us express the $0\nu 2\beta$ decay probability (neglecting right-handed contributions) as follows [2]:

$$\left(T^{0\nu}_{1/2}\right)^{-1} = G^{0\nu}_{mm}\cdot |ME|^2\cdot \langle m_\nu\rangle^2 , \qquad (1)$$

where $|ME|$ is the nuclear matrix element of the $0\nu 2\beta$ decay, and $G^{0\nu}_{mm}(Z, Q_{\beta\beta})$ is the phase space factor. Ignoring for the moment the $|ME|$ calculation [2], it is evident from (1) that for the sensitivity of the 2β decay study with a particular candidate the most important parameter is the available energy release ($Q_{\beta\beta}$). First, because the phase space integral (hence, $0\nu 2\beta$ decay rate) strongly depends on $Q_{\beta\beta}$ value (roughly as $Q^5_{\beta\beta}$). Second, the larger the 2β decay energy, the simpler – from an experimental point of view – to overcome background problems. The crucial value is 2614 keV which is the energy of the most dangerous γ's from ^{208}Tl decay (^{232}Th family). Among 35 candidates there are only six nuclei with $Q_{\beta\beta}$ larger than 2.6 MeV [23]: ^{48}Ca ($Q_{\beta\beta}$ = 4272 keV, natural abundance δ = 0.187%), ^{82}Se ($Q_{\beta\beta}$ = 2995 keV, δ = 8.73%), ^{96}Zr ($Q_{\beta\beta}$ = 3350 keV, δ = 2.80%), ^{100}Mo ($Q_{\beta\beta}$ = 3034 keV, δ = 9.63%), ^{116}Cd ($Q_{\beta\beta}$ = 2805 keV, δ = 7.49%), and ^{150}Nd ($Q_{\beta\beta}$ = 3367 keV, δ = 5.64%). The values of the phase space integral $G^{0\nu}_{mm}$ for these candidates are (in units 10^{-14} yr): 6.4 (^{48}Ca), 2.8 (^{82}Se), 5.7 (^{96}Zr), 4.6 (^{100}Mo), 4.9 (^{116}Cd), and $\approx$20 (^{150}Nd) [2]. In comparison, $G^{0\nu}_{mm}$ for ^{76}Ge is equal $\approx$0.6 (in the same units) because of the lower 2β decay energy ($Q_{\beta\beta}$ = 2039 keV). From this list ^{100}Mo and ^{116}Cd were chosen as candidates for 2β decay study with the CTF in the first phase. The main reason for the choice of ^{100}Mo – in addition to its high $Q_{\beta\beta}$ value – is the fact that the Institute for Nuclear Research (Kiev) possesses $\approx$1 kg of ^{100}Mo enriched to $\approx$99%. The ^{116}Cd was chosen because during the last decade the INR (Kiev) has developed and performed 2β decay experiments with this nuclide [24,25,9,10], which can be considered as a pilot step for the proposed project with the CTF.

3 CAMEO-I experiment with ^{100}Mo in the CTF

There are two different classes of 2β decay experiments: (a) an "active" source experiment, in which the detector

(containing 2β candidate nuclei) serves as source and detector simultaneously; (b) an experiment with "passive" source which is introduced in the detector system [1]. The sensitivity of any 2β decay apparatus is determined first, by the available source strength (mass of the source), and second, by the detector background. Another factor very essential for determining the sensitivity is the energy resolution of the detector. Indeed, for a detector with poor energy resolution the events from the high energy tail of the $2\nu2\beta$ decay distribution run into the energy window of the $0\nu2\beta$ decay peak, and therefore generate background which cannot be discriminated from the $0\nu2\beta$ decay signal, even in principle. All of the decay features are similar: the same two particles are emitted simultaneously from one point of the source, in the same energy region and with identical angular distribution. However, the better the energy resolution – the smaller the 2ν tail becomes within the 0ν interval, and thus the irreducible background becomes lower. Hence, we can conclude that the ultimate sensitivity to detect $0\nu2\beta$ decay is really limited by the energy resolution of the detector, which is the most crucial parameter for any kind of set up for 2β decay study.

For the second class of experiments the sensitivity is also restricted by the trade-off between source strength and detection efficiency. The number of 2β decay candidate nuclei can be enlarged by increasing the source thickness, which at the same time will lead to lower detection efficiency caused by absorption of electrons in the source and transformation of the measured 2β decay spectra (broadening of the peak and shifting it to lower energies).

These experimental considerations are illustrated in Fig. 1, where results of model experiments to study 2β decay of ^{100}Mo are presented. The following assumptions were accepted for simulation: mass of ^{100}Mo source is 1 kg ($\approx 6 \cdot 10^{24}$ nuclei of ^{100}Mo); measuring time is 5 years; half-life of ^{100}Mo two neutrino 2β decay $T_{1/2}(2\nu2\beta) = 10^{19}$ yr (e.g. see [26]), while for 0ν mode $T_{1/2}(0\nu2\beta) = 10^{24}$ yr. The simulations were performed with the GEANT3.21 package [27] and event generator DECAY4 [28], which describes the initial kinematics of the events in α, β, and 2β decay (how many particles are emitted, their types, energies, directions and times of emission). The initial 2β decay spectra are shown in Fig. 1a and Fig. 1b for different vertical scales. These spectra simulate 2β decay of ^{100}Mo nuclei placed in an ideal detector ("active" source technique) with 100% efficiency for 2β decay events and with zero background (energy resolution and energy threshold of 10 keV are presumed). For the next step the ^{100}Mo source was introduced in the same detector as a foil ("passive" source technique). The simulated spectra are depicted in Fig. 1c (thickness of ^{100}Mo foil is 15 mg/cm^2) and Fig. 1d (60 mg/cm^2). Finally the energy resolution of the detector ($FWHM$) was taken into account and results are shown in Fig. 1e ($FWHM = 4\%$ at 3 MeV) and Fig. 1f ($FWHM = 8.8\%$ at 3 MeV). It should be stressed that Fig. 1 represents the results of an ideal experiment, while in any real study the available results can only be worse by reason of the actual background, higher energy threshold and lower detection efficiency, etc. In fact, this

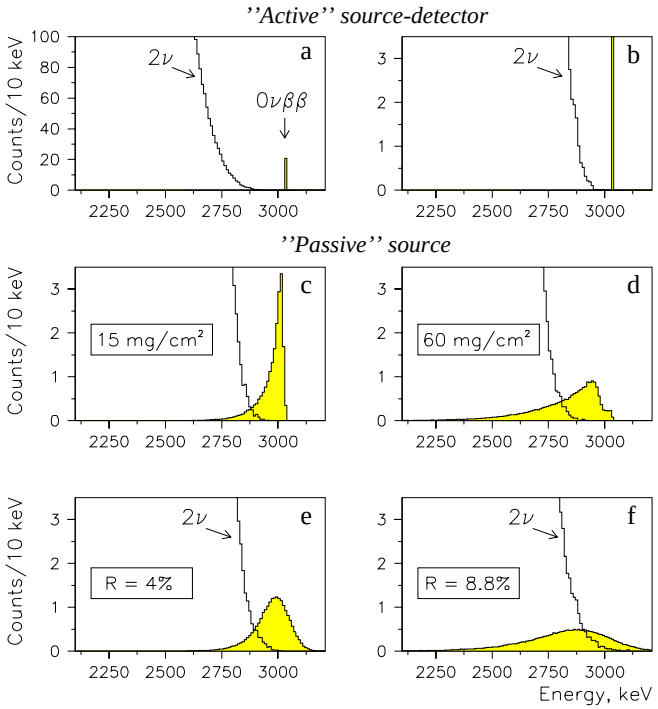

Fig. 1a–f. Simulated spectra of the model 2β decay experiment with 1 kg of ^{100}Mo. **a**, **b** "Active" source technique: ^{100}Mo nuclei in a detector with 100% efficiency, zero background, and with 10 keV energy resolution. **c**, **d** "Passive" source technique: ^{100}Mo source in the same detector with foil thickness 15 mg/cm^2 (**1c**) and 60 mg/cm^2 **1d**. **1e** The same as (**1c**) but the energy resolution ($FWHM$) of the detector at 3 MeV is 4%. **1f** The same as (**1d**) but with $FWHM = 8.8\%$

is very strong statement because it allows to set the sensitivity limit for any real apparatus. For instance, it is evident from Fig. 1f that $0\nu2\beta$ decay of ^{100}Mo with half-life $T_{1/2} = 10^{24}$ yr will hardly be observed by using the "passive" source technique with the following characteristics: (i) product of detection efficiency by number of ^{100}Mo nuclei $\approx 6 \cdot 10^{24}$ (e.g., 1 kg of ^{100}Mo at 100% efficiency, or 10 kg of ^{100}Mo at 10% efficiency); (ii) ^{100}Mo source thickness of 60 mg/cm^2; (iii) $FWHM = 8.8\%$ at 3 MeV. At the same time, it is obvious from Fig. 1e that such a goal can be reached with similar apparatus with $FWHM = 4\%$ at 3 MeV, and with a 15 mg/cm^2 source.

The last solution requires an increase of source area, which is usually limited by the available dimensions of the low background detectors used for 2β decay search. However, the unique features of the CTF – large sensitive volume and super-low background rate of the detector – permit an advanced 2β decay study of ^{100}Mo with the help of large square (≈ 7 m^2) and thin ^{100}Mo foil placed inside the liquid scintillator.

The ^{100}Mo source in the CTF is a complex system placed in the inner vessel with liquid scintillator. It can be represented by three mutually perpendicular and crossing flat disks with diameter of 180 cm whose centers are aligned with the center of inner vessel of the CTF. Each

disk is composed of three layers: inner ^{100}Mo source[2] (thickness of ≈15 mg/cm^2) placed between two plastic scintillators of 1 mm thickness. The inner side of each plastic is coated with thin Al foil serving as light reflector, while the whole source "sandwich" must be encapsulated by thin transparent film (made of teflon or syndiotactic polypropylene) to avoid plastic dissolution in liquid scintillator and a possible deterioration of the CTF performance. Plastic detectors can have a much longer decay constant (f.e. as Bicron plastic BC-444 with $\tau \approx 260$ ns and light output ≈40% of anthracene) with respect to the liquid scintillator, thus their pulses can be discriminated easily from the liquid scintillator signals. The plastics tag electrons emitted from the ^{100}Mo source, reducing the background of this complex detector system significantly. The energy loss measured by the plastics are added to the electron energy deposit in the liquid scintillator to obtain an accurate value of the electron energy and to improve the energy resolution of the whole detector.

3.1 Light collection, energy and spatial resolution

The energy resolution of the scintillation detector depends mainly on the quality of scintillator itself, the fraction of light collected by PMTs, uniformity of light collection, quantum efficiency and noise of the PMT photocathodes, stability and noise of the electronics. The excellent liquid scintillator used in the CTF yields about 10^4 emitted photons per MeV of energy deposited. In the present CTF design the actual optical coverage is 20% and the number of photoelectrons (p.e.) per MeV measured experimentally is (300 ± 30)/MeV on average. Thus with fourfold increase of light collection it would yield ≈1200 p.e. per 1 MeV or ≈3600 p.e. for 3 MeV.

To increase the actual optical coverage in the CTF, the PMTs can be mounted closer to the center of the detector. For instance, if 200 PMTs are fixed at diameter 5 m (and correspondingly the light concentrators' entrances at diameter 4 m), or 96 PMTs are fixed at diameter 3.8 m, the optical coverage is equal ≈80%. We consider below the last configuration because it is the worst case for background contribution from the PMTs[3]. Since the whole volume of the scintillator is divided by ^{100}Mo sources into 8 sectors, the PMTs are split into 8 groups of 12 PMTs each, so that one sector is viewed by one PMT group. Within the single sector (three mutually perpendicular reflector plates) scintillation photons would undergo less than 1.5 reflections on average before reaching the light concentrator aperture. The Monte Carlo simulation of the light propagation in such a geometry was performed with the help of GEANT3.21 program [27]. The emission spectrum and angular distribution of scintillation photons were added to GEANT code. The simulation finds that 3 MeV energy deposit would yield ≈3700 photoelectrons allowing a measurement of the neutrinoless 2β decay peak of ^{100}Mo ($Q_{\beta\beta}$ = 3034 keV) with an energy resolution $FWHM = 4\%$.

This goal can be reached if the non-uniformity of light collection is corrected by using accurate spatial information about each event; hence, the spatial reconstruction ability of the CTF has to be enhanced also. The results of the Monte Carlo simulation prove such a possibility and show that spatial resolution of ≈5–6 cm can be obtained with the upgraded CTF[4]. Primarily this is due to better light collection (increased by a factor of four). Secondly, it is owing to the spatial reconstruction method based on the comparison of pulse amplitudes from the different PMTs (within one group of 12 PMTs), and at the same time due to analysis of the time structure of each pulse (which can include direct and reflected light).

3.2 Background simulation

The model of the CAMEO-I set up with ^{100}Mo (described above) is used for the calculations. We distinguish here between so called "β" layers of the liquid scintillator, 15 cm thick[5] on both sides of the complex ^{100}Mo source, and the rest of the liquid scintillator volume serving as an active shield for these main inner layers. In such a detector system the following energies are measured:

i) E_1^{pl} and E_2^{pl} are the energy losses in the first and second plastic;
ii) E_1^{β} and E_2^{β} are the energy deposits in the first and second "β" layer;
iii) E^{ls} is the energy loss in the liquid scintillator active shield.

The energy threshold values of the detectors are set as E_{thr}^{pl}= 15 keV for the plastic and $E_{thr}^{ls} = E_{thr}^{\beta} = 10$ keV for the liquid scintillator. The energy resolution is $FWHM^{pl} = \sqrt{10.8 \cdot E^{pl}}$ for the plastic and $FWHM^{\beta} = \sqrt{4.8 \cdot E^{\beta}}$ for the liquid scintillator ($FWHM$, E^{pl} and E^{β} are in keV). The latter corresponds to the value of 4% at 3 MeV. The following cuts are used in the simulation in order to recognize the double β decay events:

i) E_1^{pl} or $E_2^{pl} \geq E_{thr}^{pl}$;
ii) $E_1^{pl} + E_2^{pl} \geq 300$ keV;
iii) if $E_i^{\beta} \geq E_{thr}^{\beta}$, the corresponding E_i^{pl} must be $\geq E_{thr}^{pl}$, necessarily;
iv) $E^{ls} \leq E_{thr}^{ls}$, i. e. there is no signal in the liquid scintillator active shield.

[2] In fact, in the plane of the disk the ^{100}Mo source itself consists of four sectors with spacing between them of 12 cm, which helps in spatial reconstruction when events occur near the crossing of the disks

[3] Special R&D is in progress now to find optimal solution for the required 80% optical coverage in the CTF

[4] The value obtained for the spatial resolution should be considered as indicative because in this preliminary phase of study a simplified model for light propagation in the CTF liquid scintillator has been used

[5] These "β" layers are separated from the total volume of the liquid scintillator by using the spatial information from the CTF. The thickness of 15 cm is chosen to guarantee the proper spatial reconstruction accuracy and the full absorption of the electrons emitted in the 2β decay of ^{100}Mo

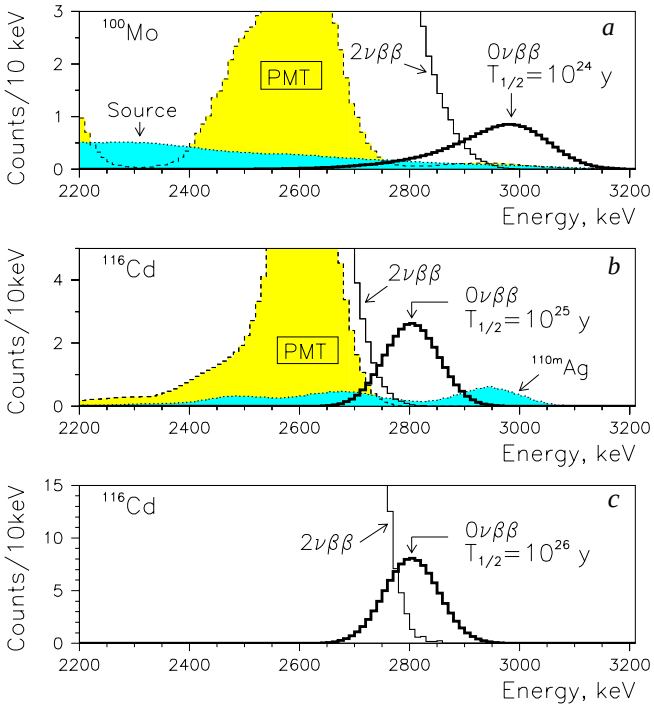

Fig. 2. a The response functions of the CTF (5 kg·yr statistics) for 2β decay of ^{100}Mo with $T_{1/2}(2\nu) = 10^{19}$ yr and $T_{1/2}(0\nu) = 10^{24}$ yr (solid histogram). Total simulated contributions due to ^{100}Mo contamination by ^{214}Bi and ^{208}Tl (dotted line), and from ^{214}Bi and ^{208}Tl in the PMTs (dashed histogram). **b** The response functions of the CTF with 65 kg of $^{116}CdWO_4$ crystals (5 yr measuring period) for 2ν2β decay of ^{116}Cd ($T_{1/2} = 2.7{\cdot}10^{19}$ yr), and 0ν2β decay with $T_{1/2} = 10^{25}$ yr (solid histogram). The simulated contribution from ^{208}Tl in the PMTs (dotted line) and from cosmogenic ^{110m}Ag (dashed histogram). **c** The response functions of the BOREXINO set up with 1 t of $^{116}CdWO_4$ crystals (10 yr measuring time) for 2ν2β decay of ^{116}Cd with $T_{1/2} = 2.7{\cdot}10^{19}$ yr, and 0ν2β decay with $T_{1/2} = 10^{26}$ yr (solid histogram)

The simulation of the background and decays of radioactive nuclides in the installation were performed with the help of GEANT3.21 [27] and the event generator DECAY4 [28].

3.2.1 Two neutrino 2β decays of ^{100}Mo

The half-life of 2ν2β decay of ^{100}Mo has been already measured as $\approx 10^{19}$ yr (e.g. [1,8,26]), hence the corresponding activity of a 1 kg ^{100}Mo source equals ≈13.2 mBq. The response functions of the CAMEO-I set up for 2ν2β decay of ^{100}Mo with $T_{1/2} = 10^{19}$ yr as well as for 0ν2β decay with $T_{1/2} = 10^{24}$ yr (for comparison) were simulated as described above, and results are depicted in Fig. 2a. The calculated values of efficiency for the neutrinoless channel are 80% (within energy window 2.8–3.15 MeV), 74% (2.85–3.15 MeV), and 63.5% (2.9–3.15 MeV). Background due to 2ν2β decay distribution are 19.7 counts (2.8–3.15 MeV), 6.1 counts (2.85–3.15 MeV), and 1.3 counts (2.9–3.15 MeV) for 5 years measuring period.

3.2.2 Radioactive contamination of the ^{100}Mo source

The ≈1 kg sample of metallic molybdenum enriched in ^{100}Mo to ≈99% – which has to be applied in the present project – was already used in the quest for 2β decay of ^{100}Mo to the excited states of ^{100}Ru [29]. In that experiment the radioactive impurities of the ^{100}Mo source by ^{40}K and nuclides from ^{232}Th and ^{238}U chains were measured. Only ^{208}Tl (measured activity is ≤ 0.5 mBq/kg) and ^{214}Bi (measured activity is (12±3) mBq/kg) – due to their high energy release – could generate the background in the 0ν2β decay energy window for ^{100}Mo. The background problem associated with ^{100}Mo radioactive contamination was carefully investigated by the NEMO collaboration, which is going to begin 2β decay measurements with ≈10 kg of ^{100}Mo [30]. It was found that for the NEMO-3 detector the maximum acceptable internal activities of ^{100}Mo are 0.3 mBq/kg for ^{214}Bi and 0.02 mBq/kg for ^{208}Tl [30]. Due to the intensive R&D performed by the NEMO collaboration [31] even lower radioactive contamination of ^{100}Mo source have been already reached by using presently available physical and chemical methods of purification: ≤ 0.2 mBq/kg for ^{214}Bi and 0.01 mBq/kg for ^{208}Tl [32]. On this basis, in our calculation the ^{100}Mo contamination criterion for ^{214}Bi has been taken as 0.3 mBq/kg, and for ^{208}Tl as 0.1 mBq/kg, which is only 5 times better than the actual activity limit in our ^{100}Mo sample (0.5 mBq/kg)[6].

The results of simulation, performed as described above, are as following: i) ^{214}Bi contribution to background within the energy interval 2.9–3.15 MeV is 6.5 counts/yr·kg; ii) ^{208}Tl contribution is equal to 0.06 counts/yr·kg. The mentioned impurities can be really dangerous for the experiment. However, there exists a possibility to reduce these background substantially by using information on the arrival time of each event for analysis and selection of some decay chains in Th and U families [24, 33]. With this aim, let us consider the ^{226}Ra chain containing ^{214}Bi: ^{222}Rn ($T_{1/2}$ = 3.82 d; Q_α = 5.59 MeV) → ^{218}Po (3.10 m; Q_α = 6.11 MeV) → ^{214}Pb (26.8 m; Q_β = 1.02 MeV) → ^{214}Bi (19.9 m; Q_β = 3.27 MeV) → ^{214}Po (164.3 μs; Q_α = 7.83 MeV) → ^{210}Pb. The great advantage of the CAMEO-I experiment is the very thin ^{100}Mo source (≈15 mg/cm^2), which allows detection of most of α and β particles emitted before or after ^{214}Bi decay, and tags the latter with the help of time analysis of the measured events. Indeed, our calculation gives the following values of the detection efficiencies: ε_1 = 55% for ^{214}Po (α particles); ε_2 = 80% for ^{214}Pb (β); ε_3 = 37% for ^{218}Po (α); ε_4 = 32% for ^{222}Rn (α). The probability to detect at least one of these decays (^{214}Po or ^{214}Pb or ^{218}Po or ^{222}Rn) can be expressed as:

$$\varepsilon = 1 - (1-\varepsilon_1)\cdot(1-\varepsilon_2)\cdot(1-\varepsilon_3)\cdot(1-\varepsilon_4).$$

[6] We have accepted the less severe and more realistic criterion for ^{208}Tl, because it was shown that chemical purification of Mo is very successful concerning ^{226}Ra chain impurities, while for ^{208}Tl the procedure is very difficult and less effective [31]

By substituting in this formula the calculated efficiency values, it yields $\varepsilon = 96.1\%$, which means that only $\approx$4% of the ^{214}Bi decays would not be tagged, i.e. ^{214}Bi contribution to background can be reduced by a factor of 25 (to the value of $\approx$0.26 counts/yr·kg). The expected total α decay rate from ^{238}U and ^{232}Th families in the entire ^{100}Mo source is $\approx$300 decays/day, however for an area of 10×10 cm it is only 0.4 decays/day, which allows use of the chains with half-life of 26.8 and 19.9 minutes for time analysis. The simulated background spectrum from the internal ^{100}Mo source contamination by the ^{214}Bi and ^{208}Tl is presented in Fig. 2a, where the total internal background rate in the energy interval 2.9–3.15 MeV is 0.3 counts/yr·kg or $\approx$1.5 counts for 5 years measuring period.

3.2.3 Cosmogenic activities in ^{100}Mo source

To estimate the cosmogenic activity produced in the ^{100}Mo foil, we used the program COSMO [34] which calculates the production of all radionuclides with half-lives in the range from 25 days to 5 million years by nucleon-induced reactions in a given target. This program takes into account the variation of spallation, evaporation, fission and peripheral reaction cross sections with nucleon energy, target and product charge and mass numbers, as well as the energy spectrum of cosmic ray nucleons near the Earth's surface.

For the CAMEO-I project cosmogenic activities were calculated for ^{100}Mo source enriched in ^{100}Mo to 98.5% (other Mo isotopes: ^{98}Mo–0.7%, ^{97}Mo–0.1%, ^{96}Mo–0.2%, ^{95}Mo–0.2%, ^{94}Mo–0.1%, ^{92}Mo–0.2%). It was assumed 5 years exposure period and deactivation time of about one year in the underground laboratory. The calculation shows that among several nuclides with $T_{1/2} \geq 25$ d produced in ^{100}Mo source only two can give some background in the energy window of the ^{100}Mo neutrinoless 2β decay. These are ^{88}Y (Q_{EC}=3.62 MeV; $T_{1/2}$=107 d) and ^{60}Co (Q_{β}=2.82 MeV; $T_{1/2}$=5.3 yr). Fortunately their activities are very low ($\approx$ 190 decays/yr for ^{88}Y and $\approx$50 decays/yr for ^{60}Co), thus the estimated background in the energy region of 2.7–3.2 MeV is practically negligible: $\leq$ 0.02 counts/yr·kg from ^{88}Y activity and $\leq$ 0.005 counts/yr·kg from ^{60}Co.

3.2.4 External background

There are several origins of the external background in the CAMEO-I experiment, for example, neutrons and γ quanta from natural environmental radioactivity (mainly from concrete walls of the Gran Sasso Underground Laboratory), contamination of PMTs by ^{40}K and nuclides from U and Th families, Rn impurities in the shielding water, cosmic muons (μ showers and muon induced neutrons, inelastic scattering and capture of muons), etc. From all of them only γ quanta caused by PMT contamination and by Rn impurities in the shielding water were simulated in the present work, while others were simply estimated as negligible on the basis of the results of [35], where such origins and contributions for the GENIUS project [36] were investigated carefully.

The radioactivity values of the EMI 9351 PMT accepted for the simulation are: 0.194 Bq/PMT (^{208}Tl); 1.383 Bq/PMT (^{214}Bi); and 191 Bq/PMT (^{40}K) [20,37]. Also possible ^{222}Rn activity $\approx$ 30 mBq/m^3 in the shielding water (in the region surrounding the inner vessel) is taken into account. The model of the CAMEO-I detector system described above was used in the calculations, but with two differences: i) "β" layers are considered as liquid scintillator blocks with dimensions 10×10×10 cm^3; ii) the threshold of the liquid scintillator active shield is increased to 30 keV. The simulation performed under these assumptions gives the following background rate in the $0\nu2\beta$ decay energy interval (2.9–3.15 MeV): i) 0.32 counts/yr· kg due to ^{214}Bi in PMT; ii) practically zero rates from ^{208}Tl in the PMTs and ^{222}Rn in the shielding water. The total simulated background contributions due to ^{214}Bi and ^{208}Tl contamination of the PMTs is shown in Fig. 2a also. After 5 years it yields $\approx$1.6 counts in the energy window 2.9–3.15 MeV. Summarizing all background sources for 5 years of measurements, one can obtain the total number of $\approx$4.4 counts in the energy range 2.9–3.15 MeV.

3.3 Sensitivity of the CAMEO-I experiment with ^{100}Mo

The sensitivity of the proposed experiment can be expressed in the term of a lower half-life limit for the $0\nu2\beta$ decay of ^{100}Mo as following:

$$T_{1/2} \geq \ln 2 \cdot N \cdot \eta \cdot t/S, \qquad (2)$$

where N is the number of ^{100}Mo nuclei ($\approx 6 \cdot 10^{24}$ in our case); t is the measuring time (5 years); η is the detection efficiency (63.5%); and S is the number of effect's events, which can be excluded with a given confidence level on the basis of measured data. Thus for the five years CAMEO-I experiment $T_{1/2} \geq (13/S) \cdot 10^{24}$ yr. Taking into account the expected background of 4.4 counts, we can accept 3–5 events as the value for S (depending on the method of estimating S [38,39]) which gives $T_{1/2} \geq$ (3–5)·10^{24} yr and, in accordance with [40], the limit on the neutrino mass $\langle m_\nu \rangle \leq 0.5$ eV. On the other hand, it is evident from Fig. 2a that neutrinoless 2β decay of ^{100}Mo with half-life $T_{1/2} = 10^{24}$ yr can certainly be registered: the signal (13 counts) to background (4.4 counts) ratio is approximately 3:1.

Similar limits $T_{1/2}(0\nu2\beta) \geq$ (3–5)·10^{24} yr can be obtained by the CAMEO-I set up with other nuclides, ^{82}Se ($Q_{\beta\beta}$ = 2996 keV), ^{96}Zr ($Q_{\beta\beta}$ = 3350 keV), ^{116}Cd ($Q_{\beta\beta}$ = 2804 keV), and ^{150}Nd ($Q_{\beta\beta}$ = 3368 keV)[7]. Due to its reasonable cost ^{116}Cd is the preferable second candidate after ^{100}Mo. Note, however, that a half-life limit of $\approx 5 \cdot 10^{24}$ yr for ^{150}Nd would lead – on the basis of the nuclear matrix

[7] We do not include ^{48}Ca ($Q_{\beta\beta}$ = 4272 keV) in that list because of its very low natural abundance (0.187%), and hence extremely high cost of a one kg ^{48}Ca source

elements calculation [40] – to a restriction on the neutrino mass $\langle m_\nu \rangle \leq 0.08$ eV.

It should be also noted, that CAMEO-I set up will allow to set a severe limits on $0\nu2\beta$ channels with emission of one or two Majorons, and to measure precisely the $2\nu2\beta$ decay rate of ^{100}Mo.

4 High sensitivity 2β decay study of ^{116}Cd with the CTF

The most sensitive $0\nu2\beta$ results are obtained by using an "active" source technique [1]. We recall the highest limits $T^{0\nu}_{1/2} \geq$ (1–2)·10^{25} yr established for ^{76}Ge with the help of high purity (HP) enriched ^{76}Ge detectors [13,14], and bounds $T^{0\nu}_{1/2} \geq \sim 10^{23}$ yr set for ^{136}Xe with a high pressure Xe TPC [12], ^{130}Te with TeO_2 low temperature bolometers [11], and ^{116}Cd with ^{116} $CdWO_4$ scintillators [10].

Continuing this line, we propose to advance the experiment with $^{116}CdWO_4$ to the sensitivity level of $\approx 10^{26}$ yr by exploiting the advantages of the CTF. The idea is to place ≈100 kg of enriched $^{116}CdWO_4$ crystals in the liquid scintillator of the CTF, which would be used as a light guide and anticoincidence shield for the main $^{116}CdWO_4$ detectors (CAMEO-II project). To prove the feasibility of this task we are considering in the following discussion a pilot ^{116}Cd experiment, and then the design concept of the present proposal, as well as problems concerning the light collection, energy and spatial resolution, background sources and sensitivity estimates of the CAMEO-II project with ^{116}Cd.

4.1 The pilot ^{116}Cd study

Here we briefly recall the main results of ^{116}Cd research performed during the last decade by the INR (Kiev)[8] in the Solotvina Underground Laboratory (in a salt mine 430 m underground [41]), and published elsewhere [24, 25,9,10]. The cadmium tungstate crystal scintillators, enriched in ^{116}Cd to 83%, were grown for research [24]. The light output of this scintillator is relatively large: ≈40% of NaI(Tl) [42]. The refractive index is 2.3. The fluorescence peak emission is at 480 nm with principal decay time of ≈14 μs [43]. The density of $CdWO_4$ crystal is 7.9 g/cm^3, and the material is non-hygroscopic and chemically inert.

In the recent phase of the experiment (from 1998) a new set up with four $^{116}CdWO_4$ crystals (total mass 339 g) was mounted in the Solotvina Laboratory [10]. The enriched detectors are viewed by a special low background 5″ EMI tube (with RbCs photocathode) through one light-guide (⌀10×55 cm), which is composed of two glued parts: quartz 25 cm long and plastic scintillator (Bicron BC-412) 30 cm long. The main detectors are surrounded by an active shield made of 15 natural $CdWO_4$ crystals of large volume [42] (total mass 20.6 kg). These are viewed by a low background PMT through an active plastic light-guide (⌀17×49 cm). The whole $CdWO_4$ array is situated within an additional active shield made of plastic scintillator 40×40×95 cm, thus, together with active light-guides, complete 4π active shielding of the main $^{116}CdWO_4$ detectors is provided. The outer passive shield consists of high-purity copper (3–6 cm), lead (22.5–30 cm) and polyethylene (16 cm). The set up is isolated carefully against penetration of air which could be contaminated by radon.

[8] From 1998 this experiment was carried out by the Kiev-Firenze collaboration [10]

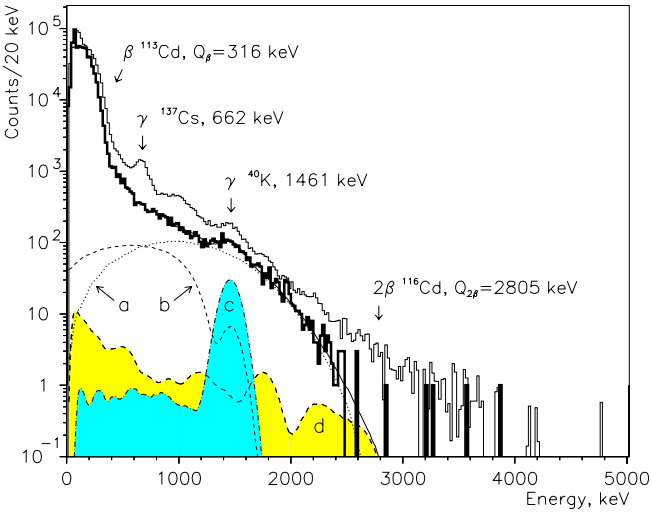

Fig. 3. Background spectrum of four enriched $^{116}CdWO_4$ crystals (339 g) measured during 4629 h (solid histogram). The old data with one $^{116}CdWO_4$ crystal (121 g; 19986 h) normalized to 339 g and 4629 h (thin histogram). The model components: (a) $2\nu2\beta$ decay of ^{116}Cd (fit value is $T_{1/2}(2\nu) = 2.6(1)\cdot10^{19}$ yr); (b) ^{40}K in the $^{116}CdWO_4$ detectors (0.8 ± 0.2 mBq/kg); (c) ^{40}K in the shielding $CdWO_4$ crystals (2.1 ± 0.3 mBq/kg); (d) ^{226}Ra and ^{232}Th in the PMTs

The multichannel event-by-event data acquisition is based on two IBM personal computers (PC) and a CAMAC crate. For each event the following information is stored on the hard disk of the first PC: the amplitude (energy), arrival time and additional tags. The second computer records the pulse shape of the $^{116}CdWO_4$ scintillators in the energy range 0.25–5 MeV [43]. Two PC-DIO-24 boards (National Instruments) are used to link both computers and establish – with the help of proper software – a one-to-one correspondence between the pulse shape data recorded by the second computer and the information stored in the first PC.

The routine calibration of the energy scale and resolution of the main detector was carried out weekly with a ^{207}Bi source and once per two weeks with ^{232}Th. In particular, the energy resolution is equal to 11.5% at 1064 keV and 8.0% at 2615 keV. Also, the relative light yield for α particles as compared with that for electrons (α/β ratio) and energy resolution were measured with α sources (outer and inner) as following: $\alpha/\beta \approx 0.15(1)$ and $FWHM_\alpha$ (keV) $= 0.053E_\alpha$ (E_α is in keV).

The background spectrum measured during 4629 h in the new set up with four $^{116}CdWO_4$ crystals [10] is given in Fig. 3, where old data obtained with one $^{116}CdWO_4$

crystal of 121 g are also shown for comparison. The background is lower in the whole energy range, except for the β spectrum of ^{113}Cd ($Q_\beta = 316$ keV)[9]. In the energy region 2.5–3.2 MeV (location of expected $0\nu2\beta$ peak) the background rate is 0.03 counts/yr·kg·keV, twenty times lower than before [24,25]. It was achieved first, due to new passive and active shielding, and secondly, as a result of the time-amplitude and pulse-shape analysis of the data.

As an example of the time-amplitude technique we consider here the analysis of the following sequence of α decays from the ^{232}Th family: ^{220}Rn ($Q_\alpha = 6.40$ MeV, $T_{1/2} = 55.6$ s) $\rightarrow$ ^{216}Po ($Q_\alpha = 6.91$ MeV, $T_{1/2} = 0.145$ s) $\rightarrow$ ^{212}Pb. The electron equivalent energy for ^{220}Rn α particles in $^{116}CdWO_4$ is $\approx$1.2 MeV, thus all events in the energy region 0.7–1.8 MeV were used as triggers. Then all signals following the triggers in the time interval 10–1000 ms (94.5% of ^{216}Po decays) were selected. The spectra of the ^{220}Rn and ^{216}Po α decays obtained in this way from data – as well as the distribution of the time intervals between the first and second events – are in an excellent agreement with those expected from α particles of ^{220}Rn and ^{216}Po [10]. It leads to the activity of ^{228}Th (^{232}Th family) inside $^{116}CdWO_4$ crystals as 38(3) μBq/kg [10].

The same technique was applied to the sequence of α decays from the ^{235}U family, and yields 5.5(14) μBq/kg for ^{227}Ac impurity in the crystals.

The pulse shape (PS) of $^{116}CdWO_4$ events (0.25–5 MeV) is digitized by a 12-bit ADC and stored in 2048 channels with 50 ns/channel width. Due to different shapes of the scintillation signal for various kinds of sources the PS technique based on the optimal digital filter was developed, and clear discrimination between γ rays and α particles was achieved [43]. In the energy region 4.5–6 MeV for α particles (or 0.8–1.2 MeV for γ quanta) numerical characteristics of the shape (shape indicator, SI) are as following: $SI_\gamma = 21.3 \pm 2.0$, and $SI_\alpha = 32.5 \pm 2.9$. The PS selection technique ensures the possibility to discriminate "illegal" events: double pulses, α events, etc., and thus suppress the background.

The results of PS analysis of the data are presented in Fig. 4. The initial (without PS selection) spectrum of the $^{116}CdWO_4$ scintillators in the energy region 1.2–4 MeV – collected during 4629 h in anticoincidence with the active shield – is depicted in Fig. 4a, while the spectrum after PS selection of the β/γ events, whose SI lie in the interval $SI_\gamma - 3.0\sigma_\gamma \leq SI \leq SI_\gamma + 2.4\sigma_\gamma$ is shown in Fig. 4b. From these figures the background reduction due to pulse-shape analysis is evident.

To estimate the half-life limits for different neutrinoless 2β decay mode, the simple background model was used. In fact, in the $0\nu2\beta$ decay energy region only three background components (presented in Fig. 3) are important: (i) external γ background from U/Th contamination of the PMTs; (ii) the tail of the $2\nu2\beta$ decay spectrum; and (iii) the internal background distribution expected from the ^{212}Bi $\rightarrow$ ^{212}Po $\rightarrow$ ^{208}Pb decay (^{228}Th chain). The limits for the neutrinoless mode of 2β decay are set

[9] Abundance of ^{113}Cd in enriched $^{116}CdWO_4$ crystals is $\approx$ 2% [24]

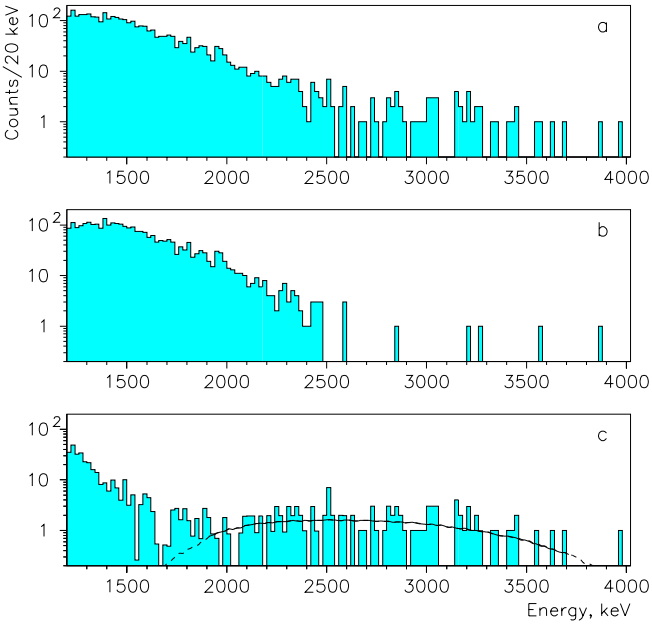

Fig. 4. **a** Initial spectrum of $^{116}CdWO_4$ crystals (339 g, 4629 h) without pulse-shape discrimination; **b** PS selected β/γ events (see text); **c** the difference between spectra in **a** and **b** together with the fit by the response function for ^{212}Bi $\rightarrow$ ^{212}Po $\rightarrow$ ^{208}Pb decay chain. The fit value of ^{228}Th activity inside $^{116}CdWO_4$ crystals is 37(4) μBq/kg

as $T_{1/2} \geq 0.7(2.5)\cdot10^{23}$ yr at 90%(68%) C.L. (for transition to the ground state of ^{116}Sn), while for decays to the first 2^+_1 and second 0^+_1 excited levels of ^{116}Sn as $T_{1/2} \geq 1.3(4.8)\cdot10^{22}$ yr and $\geq 0.7(2.4)\cdot10^{22}$ yr at 90%(68%) C.L., accordingly. For 0ν decay with emission of one or two Majorons, the limits are: $T_{1/2}(0\nu M1) \geq 3.7(5.8)\cdot10^{21}$ yr and $T_{1/2}(0\nu M2) \geq 5.9(9.4)\cdot10^{20}$ yr at 90%(68%) C.L. Also the half-life of ^{116}Cd two neutrino 2β decay is determined as $T_{1/2}(2\nu2\beta) = 2.6 \pm 0.1(\text{stat})^{+0.7}_{-0.4}(\text{syst})\cdot10^{19}$ yr [10].

The following restrictions on the neutrino mass (using calculations [40]) and neutrino-Majoron coupling constant (on the basis of calculation [44]) are derived from the experimental results obtained: $m_\nu \leq 2.6(1.4)$ eV and $g_M \leq 12(9.5)\cdot10^{-5}$ at 90%(68%) C.L. [10]. It is expected that after $\approx$5 years of measurements a neutrino mass limit of $m_\nu \leq 1.2$ eV would be found. However further advance of this limit to the sub-eV neutrino mass domain is impossible without substantial sensitivity enhancement, which can be reached with a larger number of $^{116}CdWO_4$ detectors placed in the liquid scintillator of the CTF.

4.2 Design concept of the CAMEO-II project with ^{116}Cd

In the preliminary design concept of the CAMEO-II experiment, $\approx$50 enriched $^{116}CdWO_4$ crystals of large volume ($\approx$350 cm^3) are located in the liquid scintillator of the CTF and fixed at 0.4 m distance from the CTF center, thus homogeneously spread out on a sphere with diame-

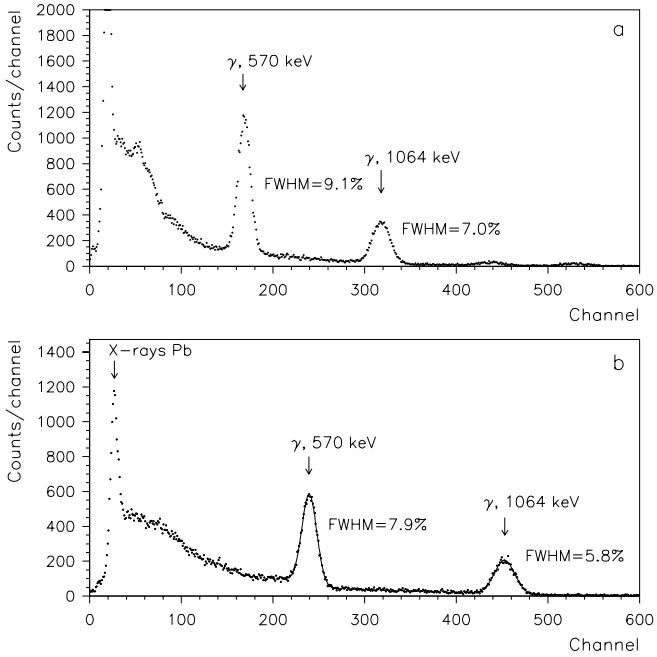

Fig. 5a,b. The energy spectra of a ^{207}Bi source measured by a $CdWO_4$ crystal ($\oslash 40 \times 30$ mm) for two arrangements: **a** standard, where the $CdWO_4$ crystal wrapped by teflon diffuser is directly coupled to the PMT's photocathode with optical glue; **b** the $CdWO_4$ crystal is located in liquid and viewed by two distant PMTs (see text)

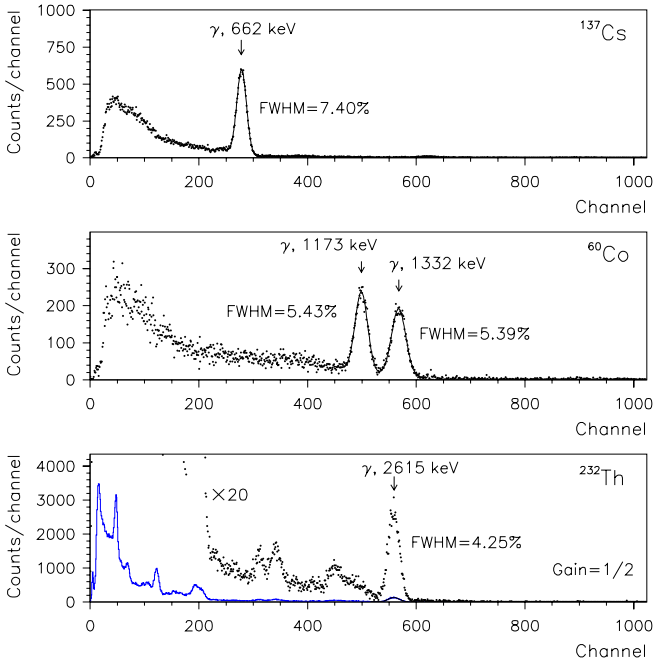

Fig. 6. The energy spectra of ^{137}Cs, ^{60}Co and ^{232}Th sources measured by a $CdWO_4$ crystal ($\oslash 40 \times 30$ mm) placed in liquid and viewed by two distant PMTs

ter 0.8 m. With a mass of 2.7 kg per crystal ($\oslash 7 \times 9$ cm) the total number of ^{116}Cd nuclei is $\approx 2 \times 10^{26}$. It is proposed that 200 PMTs with light concentrators are fixed at diameter 5 m providing the total optical coverage of 80% (see footnote 3).

The light output of $CdWO_4$ scintillator is (35–40)% of NaI(Tl) which yields $\approx 1.5 \cdot 10^4$ emitted photons per MeV of energy deposited. With a total light collection of ≈80% and PMT quantum efficiency of ≈25% energy resolution of ≈4% at ≈ 3 MeV can be obtained.

To justify this value a GEANT Monte Carlo simulation of the light propagation in this geometry was performed, which gave ≈4000 photoelectrons for 2.8 MeV energy deposit. Therefore, with total optical coverage 80% the neutrinoless 2β decay peak of ^{116}Cd ($Q_{\beta\beta} = 2805$ keV) can be measured with energy resolution $FWHM = 4\%$. The principal feasibility to obtain such an energy resolution with $CdWO_4$ crystal situated in a liquid has been demonstrated by measurements with the help of a simple device. A cylindrical $CdWO_4$ crystal (40 mm in diameter and 30 mm in height) was fixed in the centre of a teflon container with inner diameter 70 mm. This was coupled on opposite sides with two PMTs Philips XP2412, so that the distance from each flat surface of crystal to the corresponding PMT's photocathode is 30 mm, while the gap between the side surface of the crystal and the inner surface of the container is 15 mm. The container was filled up with the pure and transparent paraffin oil[10] (refractive index ≈1.5). Two PMTs work in coincidence and results of measurements with ^{207}Bi source are depicted in Fig. 5, where the spectrum obtained with the standard detector arrangement ($CdWO_4$ crystal wrapped by teflon diffuser and directly coupled to the PMT's photocathode with optical glue) is also shown for comparison. As evident from Fig. 5, a substantial (≈42%) increase in light collection was obtained with $CdWO_4$ in the liquid. It resulted in improvement of the detector energy resolution in the whole energy region 50–3000 keV (see Fig. 6 where the spectra measured with ^{137}Cs, ^{60}Co and ^{232}Th sources are presented). It should be stressed that $FWHM$ values (7.4% at 662 keV; 5.8% at 1064 keV; 5.4% at 1173 keV and 4.3% at 2615 keV) are similar to those for NaI(Tl) crystals and have never been reached before with $CdWO_4$ crystal scintillators [42].

Moreover, a strong dependence of the light collected by each individual PMT versus position of the emitting source in the crystal was found. Such a dependence can be explained by the large difference of the refraction indexes of $CdWO_4$ crystal ($n = 2.3$) and liquid scintillator ($n' = 1.51$), which leads to light redistribution between reflection and refraction processes due to changes of the source's position.

General formulae for the angular distribution of the light emitted in the crystal and propagating in the liquid

[10] Recently these measurements were repeated with $CdWO_4$ crystal placed in the liquid scintillator on the basis of pseudocumene (used in the CTF). The results (light output and energy resolution improvements) are the same as with paraffin oil

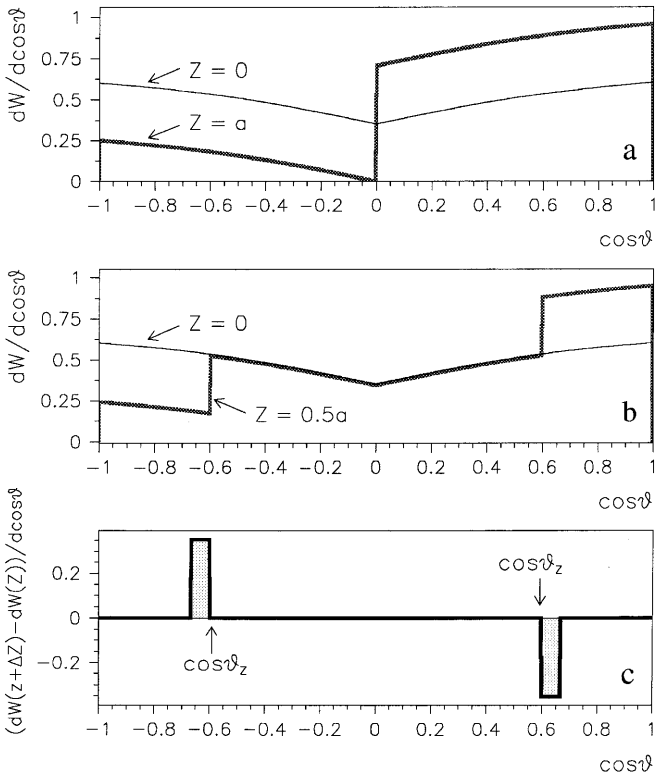

Fig. 7a–c. **a** Angular distribution of the light emitted in the $CdWO_4$ crystal and propagating in the liquid scintillator, when a light source is on the crystal axis in the center and on the bottom of the crystal (solid line). **b** The same as **a** but with a light source positioned on an arbitrary point of the axis with coordinate z. **c** The difference between angular distributions for two points on the axis with coordinates z and $(z + \triangle z)$

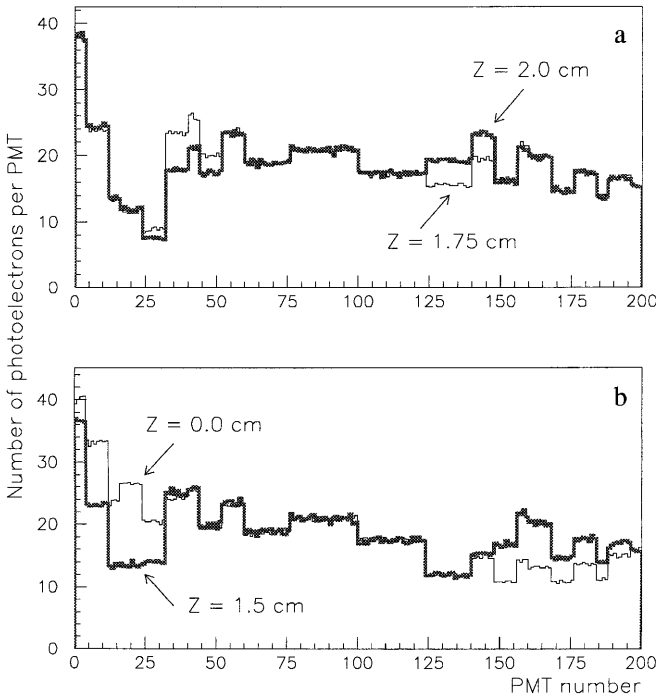

Fig. 8a,b. Simulated distributions of the photoelectron numbers among PMTs due to scintillations in $CdWO_4$ crystal ($\oslash 7 \times 9$ cm) placed in the CTF. The distance between source positions on the crystal axis equals $\triangle z = 2.5$ mm **a**, and $\triangle z = 1.5$ cm **b**

scintillator are quite cumbersome, and below we give expressions for some simple cases, when a $CdWO_4$ crystal with equal diameter and height ($d = h = 2a$) is placed in the center of the CTF detector and a light source is positioned on the crystal axis. Assuming a ratio of refraction indexes $n/n' = \sqrt{2}$ (which is close to the real value) and neglecting light absorption, the equation for the particular case with light source in the center of crystal is of the form:

$$\frac{dW}{d\cos\theta} = \frac{1}{2\sqrt{2}} \cdot \left[\frac{|\cos\theta|}{\sqrt{1+\cos^2\theta}} + 1\right], \qquad (3)$$

where θ is the angle between the axis of the crystal (z-axis in our coordinate system) and direction of the photon in the liquid scintillator. This function is depicted in Fig. 7a together with the distribution for another case with the light source on the bottom of crystal (on the axis again):

$$\frac{dW}{d\cos\theta} = \frac{1}{2\sqrt{2}} \cdot \left[\frac{|\cos\theta|}{\sqrt{1+\cos^2\theta}} + 2\Theta(\theta)\right], \qquad (4)$$

where $\Theta(\theta)$ is the unit step function depending on angle θ, as following:

$$\Theta(\theta) = \begin{cases} 1, & 0 \le \theta \le \pi/2 \\ 0, & \pi/2 < \theta \le \pi \end{cases}.$$

The angular distribution for a more general case, when the light source is positioned on an arbitrary point of the axis with coordinate z $(-a \le z \le a)$, is shown in Fig. 7b. When the location of the source is shifted from z to $z + \triangle z$, the values of angles θ_z and $\pi - \theta_z$, for which $dW/d\cos\theta$ changes sharply, are also changed: $\cos\theta_z = \sqrt{2(a-|z|)^2/(a^2+(a-|z|)^2)}$. The difference $dW(z+\triangle z)/d\cos\theta - dW(z)/d\cos\theta$ represented in Fig. 7c behaves as two peaks. The area of both peaks is equal to $\triangle S = a^2\triangle z/\left[a^2+(a-|z|)^2\right]^{3/2}$. Assuming that N is the full number of photoelectrons detected by all PMTs, and $\triangle N$ is the difference of the number of photoelectrons due to the source shift $\triangle z$, we find $\triangle N = N \cdot a^2\triangle z/[a^2+(a-|z|)^2]^{3/2}$. From the last expression one gets the formula for the spatial resolution in the $CdWO_4$ crystal by supposing that difference $\triangle N$, which can be registered with 95% C.L., is equal $\triangle N = 2\sqrt{N}$:

$$\triangle z = \frac{2a}{\sqrt{N}} \cdot \left\{1 + \left[1 - \frac{|z|}{a}\right]^2\right\}^{3/2}. \qquad (5)$$

Substituting in (5) the crystal's dimensions $a = 4$ cm, and the total number of photoelectrons $N = 4000$ yields spatial resolution of ≈ 4 mm in the center of the crystal ($z = 0$) and ≈ 1.5 mm near the top or bottom of the crystal ($z = \pm a$). Our GEANT Monte Carlo simulation proves these values and shows that, with a cylindrical $CdWO_4$ crystal ($\oslash 7 \times 9$ cm) viewed by 200 PMTs, spatial resolution of 1–5 mm can be reached depending on the event's location and the energy deposited in the

crystal (see, however, footnote 4). The simulated distributions of the photoelectron number among PMTs due to scintillations in $CdWO_4$ crystal are depicted in Fig. 8. The distance between the source's positions on the crystal axis is equal to $\triangle z = 2.5$ mm (Fig. 8a), and $\triangle z = 1.5$ cm (Fig. 8b).

These interesting features of light collection from $^{116}CdWO_4$ in the CTF would allow a reduction in the contribution from high energy γ quanta (e.g. ^{208}Tl) to background in the energy region of interest. Besides, the non-uniformity of light collection can be accurately corrected by using spatial information about each event in the $CdWO_4$ crystal, hence, helping to reach the required energy resolution of the detectors.

4.3 Background simulation

The background simulations for the CAMEO-II experiment with ^{116}Cd were performed with the GEANT code and event generator DECAY4, and by using the model described above.

4.3.1 Two neutrino 2β decays of ^{116}Cd

The half-life of two neutrino 2β decay of ^{116}Cd has been measured as $\approx 2.7 \cdot 10^{19}$ yr [45,24,10]. The response functions of the CAMEO-II set up for $2\nu2\beta$ decay of ^{116}Cd with $T_{1/2} = 2.7 \cdot 10^{19}$ yr, as well as for $0\nu2\beta$ decay with $T_{1/2} = 10^{25}$ yr were simulated, and results are depicted in Fig. 2b. The calculated values of efficiency for the neutrinoless channel are 86.1% (for energy window 2.7–2.9 MeV), and 75.3% (2.75–2.9 MeV). Background in the corresponding energy interval from $2\nu2\beta$ decay distribution is 2.3 counts/yr (2.7–2.9 MeV) or 0.29 counts/yr (2.75–2.9 MeV).

4.3.2 Radioactive contamination of $^{116}CdWO_4$ crystals

The very low levels of radioactive impurities by ^{40}K and nuclides from natural radioactive chains of ^{232}Th and ^{238}U in the enriched and natural $CdWO_4$ crystals were demonstrated by the INR (Kiev) experiment [42]. On this basis the contamination criterion for ^{214}Bi and ^{208}Tl has been accepted in our calculation as ≈ 10 μBq/kg, which is equal to the actual activity value or limit determined for different samples of $CdWO_4$ crystals [42].

The calculated background contribution from the sum of ^{208}Tl and ^{214}Bi activities is $\approx$2000 counts/yr in the energy interval 2.7–2.9 MeV. However, applying the time-amplitude analysis with spatial resolution and pulse-shape discrimination technique developed [24,10] this background rate can be reduced to $\approx$0.2 counts/yr or $\approx$1.0 counts for 5 years measuring period.

4.3.3 Cosmogenic activities in $^{116}CdWO_4$

For the CAMEO-II project cosmogenic activities in the $^{116}CdWO_4$ detectors were calculated by the program COSMO [34]. A 1 month exposure period on the Earth's surface was assumed and a deactivation time of about three years in the underground laboratory. Only two nuclides produce background in the energy window of the ^{116}Cd neutrinoless 2β decay. These are ^{110m}Ag (Q_β=3.0 MeV; $T_{1/2}$=250 d) and ^{106}Ru ($Q_\beta \approx 40$ keV; $T_{1/2}$=374 d) $\rightarrow$ ^{106}Rh (Q_β=3.5 MeV; $T_{1/2}$=30 s). Fortunately ^{106}Ru activity is low and, because the time-amplitude analysis can be applied ($T_{1/2}$=30 s), its estimated background is practically negligible: $\approx$0.1 counts/yr in the energy region 2.7–2.9 MeV, and 0.05 counts/yr (2.75–2.9 MeV). The background from ^{110m}Ag is quite large: $\approx$23 (or $\approx$20) counts/yr for the energy interval 2.7–2.9 MeV (2.75–2.9 MeV). However its contribution can be reduced significantly by using spatial information because ^{110m}Ag decays are accompanied by cascades of γ quanta with energies $\geq$ 600 keV, which would be absorbed in spatially separated parts of the detector giving an anticoincidence signature. Simulation under the assumption that the $^{116}CdWO_4$ crystal consists of small independent detectors with $h = d = 1.2$ cm, yields the residual background rates $\approx$0.3 (or 0.2) counts/yr in the corresponding energy region 2.7–2.9 MeV (2.75–2.9 MeV). The simulated spectrum from the cosmogenic activity of ^{110m}Ag is depicted in Fig. 2b.

4.3.4 External background

As in the previous case with ^{100}Mo, from the various sources of external background only γ quanta due to PMT contamination and from Rn impurities in the shielding water were simulated, while others were estimated as negligible on the basis of the results of ref. [35]. The radioactivity values of the EMI 9351 PMT accepted for the simulation are: 0.194 Bq/PMT for ^{208}Tl; 1.383 Bq/PMT for ^{214}Bi; and 191 Bq/PMT for ^{40}K [20,37]. Also possible ^{222}Rn activity in the shielding water (in the region surrounding the inner vessel) at the level of $\approx$30 mBq/m^3 was taken into account. The simulation performed under these assumptions finds that the only important contribution to the background in the vicinity of the $0\nu2\beta$ decay energy is ^{208}Tl activity from the PMTs. The calculated values are $\approx$0.8 and 0.05 counts/yr in the energy interval 2.7–2.9 MeV (2.75–2.9 MeV). However, with the help of spatial information available for each event occurring inside the $^{116}CdWO_4$ crystal, these contributions can be reduced further to the level of $\approx$0.08 (or 0.005) counts/yr in the energy region 2.7–2.9 MeV (2.75–2.9 MeV). The simulated background contribution from ^{208}Tl contamination of the PMTs is shown in Fig. 2b. Summarizing all background sources gives $\approx$3 counts/yr (0.6 counts/yr) in the energy interval 2.7–2.9 MeV (2.75–2.9 MeV).

4.4 Sensitivity of the ^{116}Cd experiment

As earlier we will estimate the sensitivity of the CAMEO-II experiment with the help of (2). Taking into account the number of ^{116}Cd nuclei ($\approx 2 \times 10^{26}$), measuring time of 5 years, detection efficiency of 75%, and with expected

background of 3–4 counts, one can obtain a half-life limit $T_{1/2}(0\nu2\beta) \geq 10^{26}$ yr. On the other hand, it is evident from Fig. 2b that neutrinoless 2β decay of ^{116}Cd with half-life of $\approx 10^{25}$ yr would be clearly registered. It should be noted that such a level of sensitivity for $0\nu2\beta$ decay cannot be reached in the presently running 2β decay experiments (perhaps only with ^{76}Ge), as well as for approved projects, like NEMO-3 [30] and CUORICINO [46], which are under construction now.

The CAMEO-II experiment has an important advantage because signaling from the $^{116}CdWO_4$ crystals to the PMTs (placed far away from crystals) is provided by light propagating in the super-low background medium of liquid scintillator, whereas any other detectors must be connected with receiving modules by cables. These additional materials (wires, insulators, etc.), whose radioactive contamination are much larger in comparison with crystals or liquid scintillators, must be introduced in the neighborhood of the main detectors, giving rise to additional background[11].

Another advantage of the CAMEO-II is its simplicity and reliability, therefore experiment with $^{116}CdWO_4$ crystals can run for decades without problems and with very low maintenance cost[12].

The CAMEO-II project can be advanced farther by exploiting one ton of $^{116}CdWO_4$ detectors ($\approx 1.5 \cdot 10^{27}$ nuclei of ^{116}Cd) and the BOREXINO apparatus (CAMEO-III). With this aim 370 enriched $^{116}CdWO_4$ crystals (2.7 kg mass of each) would be placed at a diameter 3.2 m in the BOREXINO liquid scintillator. The simulated response functions of such a detector system for $2\nu2\beta$ decay of ^{116}Cd with $T_{1/2} = 2.7 \cdot 10^{19}$ yr, as well as for $0\nu2\beta$ decay with $T_{1/2} = 10^{26}$ yr considering a 10-year measuring period are depicted in Fig. 2c. Because background in BOREXINO should be even lower than in the CTF, the sensitivity of CAMEO-III for neutrinoless 2β decay of ^{116}Cd is estimated as $T_{1/2} \geq 10^{27}$ yr, while $0\nu2\beta$ decay with half-life of $\approx 10^{26}$ yr can be detected. On the basis of the half-life limit $T^{0\nu}_{1/2} \geq 10^{27}$ yr and using calculations [40,48] one can derive a limit on the neutrino mass of ≈ 0.02 eV, which is of utmost importance in the light of the current theoretical and experimental status of modern astroparticle physics [1,2,15–17].

It should be stressed that solution of the technical tasks required for the CAMEO project seems to be quite realistic – in fact, the super-low background apparatus needed for this experiment is already running (it is the CTF) or under construction (BOREXINO).

[11] There are two origins of such a background: i) radioactive contamination of the materials introduced; ii) external background penetrating through the slots in the detector shielding required for the connecting cables

[12] It should be noted that the $^{116}CdWO_4$ crystals produced for the CAMEO-II experiment can also be used as cryogenic detectors with high energy resolution [47]. In the event of a positive effect seen by CAMEO-II these crystals could be measured by the CUORE apparatus; in some sense both projects are complementary

5 Conclusions

1. The unique features of the CTF and BOREXINO (super-low background and large sensitive volume) are used to develop a realistic, competitive, and efficient program for high sensitivity 2β decay research (CAMEO project). This program includes three natural steps, and each of them would bring substantial physical results:
   CAMEO-I. With a passive 1 kg source made of ^{100}Mo and located in the liquid scintillator of the CTF, the sensitivity (in terms of the half-life limit for $0\nu2\beta$ decay) is $\approx 4 \times 10^{24}$ yr. It corresponds to a bound on the neutrino mass $m_\nu \approx 0.3$ eV.
   CAMEO-II. With ≈ 50 enriched $^{116}CdWO_4$ crystal scintillators (total mass of ≈ 100 kg) placed as "active" detectors in the liquid scintillator of the CTF the sensitivity would be $\approx 10^{26}$ yr. Pilot ^{116}Cd research, performed by the INR (Kiev) during the last decade, as well as Monte Carlo simulation show the feasibility of CAMEO-II, which will yield a limit on the neutrino mass $m_\nu \approx 0.06$ eV.
   CAMEO-III. By exploiting one ton of $^{116}CdWO_4$ detectors (370 enriched $^{116}CdWO_4$ crystals) introduced in the BOREXINO liquid scintillator, the half-life limit can be advanced to the level of $\approx 10^{27}$ yr, corresponding to a neutrino mass bound of ≈ 0.02 eV.
2. The CAMEO project has three principal advantages:
   i) Practical realization of the CAMEO project is relatively simple due to the use of already existing super-low background CTF or (presently under construction) BOREXINO apparatus;
   ii) Signaling from the $^{116}CdWO_4$ crystals to PMT (placed far away) is provided by light propagating in the high-purity medium of liquid scintillator – this allows practically zero background to be reached in the energy region of the $0\nu2\beta$ decay peak;
   iii) Extreme simplicity of the technique used for 2β decay study leads to high reliability and low maintenance costs for the CAMEO experiment, which therefore can run permanently and stably for decades.
3. Fulfillment of the CAMEO program would be a real breakthrough in the field of 2β decay investigation, and will bring outstanding results for particle physics, cosmology and astrophysics. Discovery of neutrinoless 2β decay will clearly and unambiguously manifest new physical effects beyond the Standard Model. In the event of a null result, the limits obtained by the CAMEO experiments would yield strong restrictions on parameters of manifold extensions of the SM (neutrino mass and models; dark matter and solar neutrinos; right-handed contributions to weak interactions; leptoquark masses; bounds for parameter space of SUSY models; neutrino-Majoron coupling constant; composite heavy neutrinos; Lorentz invariance, etc.), which will help to advance basic theory and our understanding of the origin and evolution of the Universe.

References

1. M. Moe, P. Vogel, Ann. Rev. Nucl. Part. Sci. **44**, 247 (1994); V.I. Tretyak, Yu.G. Zdesenko, At. Data Nucl. Data Tables **61**, 43 (1995)
2. A. Faessler, F. Simkovic, J. Phys. G: Nucl. Part. Phys. **24**, 2139 (1998); H.V. Klapdor-Kleingrothaus, Int. J. Mod. Phys. A **13**, 3953 (1998); J. Suhonen, O. Civitarese, Phys. Rep. **300**, 123 (1998)
3. J. Schechter, J.W.F. Valle, Phys. Rev. D **25**, 2951 (1982)
4. Proceedings of the Neutrino'98: Nucl. Phys. B (Proc. Suppl.) **77** (1999)
5. Y. Fukuda et al., Phys. Rev. Lett. **81**, 1562 (1998)
6. C. Athanassopoulos et al., Phys. Rev. Lett. **77**, 3082 (1996); D. H. White et al., Nucl. Phys. B (Proc. Suppl.) **70**, 207 (1999)
7. S.R. Elliot et al., Phys. Rev. C **46**, 1535 (1992)
8. N. Kudomi et al., Nucl. Phys. A **629**, 527c (1998)
9. F.A. Danevich et al., Nucl. Phys. B (Proc. Suppl.) **70**, 246 (1999)
10. F.A. Danevich et al., nucl-ex/0003001, Phys. Rev. C **62**, 045501 (2000)
11. A. Alessandrello et al., Phys. Lett. B **433**, 156 (1998)
12. R. Luescher et al., Phys. Lett. B **434**, 407 (1998)
13. L. Baudis et al., Phys. Rev. Lett. **83**, 41 (1999)
14. C.E. Aalseth et al., Phys. Rev. C **59**, 2108 (1999)
15. H.V. Klapdor-Kleingrothaus et al., hep-ph/0003219 29 Mar 2000
16. P. Vogel, nucl-th/0005020 9 May 2000
17. K. Zuber, Phys. Rep. **305**, 295 (1998)
18. G. Bellini (for the Borexino Collaboration), Nucl. Phys. B (Proc. Suppl.) **48**, 363 (1996)
19. G. Alimonti et al., Nucl. Instrum. Meth. A **406**, 411 (1998)
20. G. Alimonti et al., Astroparticle Phys. **8**, 141 (1998)
21. M. Balata et al., Nucl. Instrum. Meth. A **370**, 605 (1996)
22. G. Alimonti et al., Nucl. Instrum. Meth. A **440**, 360 (2000)
23. G. Audi, A.H. Wapstra, Nucl. Phys. A **595**, 409 (1995)
24. F.A. Danevich et al., Phys. Lett. B **344**, 72 (1995); A.Sh. Georgadze et al., Phys. At. Nucl. **58**, 1093 (1995)
25. F.A. Danevich et al., Nucl. Phys. A **643**, 317 (1998)
26. D. Dassie et al., Phys. Rev. D **51**, 2090 (1995)
27. R. Brun et al., CERN Program Library Long Write-up W5013, CERN, 1994
28. O.A. Ponkratenko et al., Phys. At. Nucl. **63**, 1282 (2000)
29. D. Blum et al., Phys. Lett. B **275**, 506 (1992)
30. F. Piquemal (for the NEMO Collaboration), Nucl. Phys. B (Proc. Suppl.) **77**, 352 (1999)
31. Proc. of the NEMO Coll. Meeting. Oleron, France, 27-30 April 1998, 408 p
32. NEMO Collaboration, hep-ex/0006031 26 Jun 2000
33. F.A. Danevich et al., Nucl. Phys. B (Proc. Suppl.) **48**, 235 (1996)
34. C.J. Martoff, P.D. Lewin, Comp. Phys. Comm. **72**, 96 (1992)
35. O.A. Ponkratenko, V.I. Tretyak, Yu.G. Zdesenko, in Proc. of Int. Conf. on Dark Matter in Astro and Part. Physics. Heidelberg, Germany 20–25 July 1998, eds. H.V. Klapdor-Kleingrothaus, L. Baudis (IOP, Bristol and Philadelphia, 1998), p. 738
36. H.V. Klapdor-Kleingrothaus et al., J. Phys. G: Nucl. Part. Phys. **24**, 483 (1998)
37. B. Caccianiga, M.G. Giammarchi, Astroparticle Phys. **14**, 15 (2000)
38. Particle Data Group, Review of Particle Physics, Phys. Rev. D **54**, 1 (1996)
39. Particle Data Group, Review of Particle Physics, Eur. Phys. J. C **3**, 1 (1998)
40. A. Staudt et al., Europhys. Lett. **13**, 31 (1990)
41. Yu.G. Zdesenko et al., in Proc. 2nd Int. Symp. Underground Physics. Baksan Valley, 1987 (Moscow, Nauka, 1988), p. 291
42. A.Sh. Georgadze et al., Instr. Exp. Technique **39**, 191 (1996); S.Ph. Burachas et al., Nucl. Instrum. Meth. A **369**, 164 (1996)
43. T. Fazzini et al., Nucl. Instrum. Meth. A **410**, 213 (1998)
44. M. Hirsch et al., Phys. Lett. B **372**, 8 (1996)
45. H. Ejiri et al., J. Phys. Soc. Japan **64**, 339 (1995)
46. E. Fiorini, Phys. Rept. **307**, 309 (1998)
47. A. Alessandrello et al., Nucl. Phys. B (Proc. Suppl.) **35**, 394 (1994)
48. R. Arnold et al., Z. Phys. C **72**, 239 (1996)